Am. J. Hum. Genet. 72:549–560, 2003

Accumulation of Mitochondrial DNA Mutations in Human Immunodeficiency Virus–Infected Patients Treated with Nucleoside-Analogue Reverse-Transcriptase Inhibitors

Annalise M. Martin,[1,*] Emma Hammond,[1,*] David Nolan,[1] Craig Pace,[1] Marion Den Boer,[3] Louise Taylor,[1] Hannah Moore,[1] Olga Patricia Martinez,[2,4] Frank T. Christiansen,[2,4] and Simon Mallal[1,2]

[1]Centre for Clinical Immunology and Biomedical Statistics, Murdoch University, and [2]Department of Clinical Immunology and Biochemical Genetics, Royal Perth Hospital, Perth, Australia; [3]TNO Protection and Health, Leiden, The Netherlands; and [4]Department of Pathology, University of Western Australia, Nedlands, Australia

Nucleoside reverse-transcriptase inhibitor (NRTI) therapy for human immunodeficiency virus (HIV) infection has been associated with mitochondrial DNA (mtDNA) polymerase-γ inhibition and subsequent mtDNA depletion. Effects on mtDNA mutation, although suggested by critical involvement of polymerase-γ in DNA-repair reactions, are unknown. In the present study, we assessed the nature and frequency of mitochondrial genome sequence differences in peripheral-blood samples taken prior to NRTI therapy and after 6–77 mo of treatment in 16 NRTI-treated patients. Samples from 10 HIV-infected, treatment-naive control individuals were taken at similar time intervals. Single-stranded conformation polymorphism (SSCP) and DNA-sequencing analysis techniques were used to detect mitochondrial genome sequence variants between paired longitudinal samples, and heteroplasmic populations were quantified after cloning and repeat SSCP/sequencing. Of 16 individuals treated with NRTIs, 5 exhibited altered SSCP profiles associated with the development of novel heteroplasmic DNA sequence changes, whereas no SSCP pattern change within these regions was observed in the control individuals. Heteroplasmic sequence changes were distributed across four regions of the genome: the noncoding region to 12S ribosomal RNA, reduced-nicotinamide-adenine-dinucleotide dehydrogenase 1, and cytochrome oxidase subunits I and III. Of the total of 26 patients who were examined in the present study, 4 of 5 patients with detectable mtDNA sequence changes since commencement of therapy developed evidence of peripheral fat wasting (lipoatrophy) between sample intervals ($P = .031$). One patient, without detectable sequence changes on NRTI therapy, also developed lipoatrophy. Levels of mtDNA copies/cell in blood samples were determined by quantitative PCR for 11 of the 16 NRTI-exposed patients; 7 of these 11 patients showed reduced levels of mtDNA in blood after therapy, including all 3 patients tested with evidence of mtDNA sequence changes on therapy. These data indicate that NRTI therapy provides conditions permissive for the development of peripheral-blood mtDNA mutations in vivo.

Introduction

Nucleoside-analogue reverse-transcriptase inhibitors (NRTIs) were the first agents to be utilized in the clinical treatment of HIV infection and continue to be incorporated into contemporary highly active therapy regimens that may combine NRTI drugs with either HIV protease inhibitors or nonnucleoside reverse-transcriptase inhibitors. Use of these highly effective regimens has allowed profound suppression of HIV viral replication, greatly reducing morbidity and mortality attributable to HIV-induced immune deficiency (Palella et al. 1998). In this setting, however, a comprehensive understanding of the potential that long-term use of antiretroviral drugs result in adverse effects, including those specifically associated with NRTI therapy (Kakuda 2000; White 2001), assumes greater importance.

NRTI drugs are nucleoside substrates for the DNA polymerase activity of HIV reverse transcriptase, acting as DNA chain terminators because of the modification of their 3′-hydroxyl group required for nucleoside attachment. In addition to the target viral polymerase, these compounds also have the capacity to inhibit mtDNA polymerase-γ, which, unlike nuclear DNA (nDNA) polymerases, is unable to discriminate effectively in favor of endogenous nucleosides in the presence of NRTIs (Longley et al. 1998). Polymerase-γ is the sole mtDNA polymerase and is therefore critical

Received October 10, 2002; accepted for publication December 2, 2002; electronically published February 13, 2003.

Address for correspondence and reprints: Prof. Simon Mallal, Centre for Clinical Immunology and Biomedical Statistics, Murdoch University, Perth, Western Australia, 6150. E-mail: S.Mallal@murdoch.edu.au

* The first two authors contributed equally to this work.

0002-9297/2003/7203-0006$15.00

for synthesis, as well as repair, of the mitochondrial-encoded genes required for oxidative phosphorylation and mitochondrial protein synthesis. Hence, maintenance of bioenergetic function in all metabolically active cells, including postmitotic cells in which nDNA synthesis is negligible, requires ongoing uptake and polymerase-γ–dependent utilization of nucleosides by mitochondria.

The proposal that NRTI-induced polymerase-γ inhibition represents a common pathway of tissue-specific adverse effects of this drug class has been presented by Lewis and Dalakas (1995). More recently, Brinkman et al. (1998) have suggested that this process may be relevant to the pathogenesis of a lipodystrophy syndrome highly prevalent in antiretroviral therapy (ART) recipients. According to this model, cellular—and ultimately organ—toxicity is proposed to be the consequence of loss of mitochondrial bioenergetic function, once mtDNA synthesis has fallen to a level incompatible with cellular viability. In vitro studies have provided important information regarding the possibility that select NRTI drugs cause DNA polymerase-γ inhibition and mtDNA depletion (Martin et al. 1994; Johnson et al. 2001; Birkus et al. 2002). A consistent ranking has emerged from these studies, with greatest potency of mtDNA synthesis inhibition attributed to zalcitabine, followed by didanosine, stavudine, and zidovudine (in that order) and, finally, by lamivudine, abacavir, and tenofovir (to an equal degree) (Kakuda 2000).

Research to date has focused primarily on mtDNA depletion as a product of mitochondrial polymerase-γ inhibition. However, it has also been recognized that NRTI therapy may also be associated with increased risk of mtDNA mutation (Lewis et al. 2001), the pathogenesis of which is likely to be multifactorial, involving increased oxidative stress and defective repair.

In the present study, we investigated the impact that NRTI therapy had on the development of peripheral-blood mtDNA mutations in 16 HIV-infected individuals, by comparing the levels of heteroplasmy in samples obtained prior to the commencement of ART and after 6–77 mo of treatment. A reference group of 10 HIV-infected, ART-naive individuals was also studied, with paired samples obtained over a similar time period. SSCP was used for mutation screening across the entire mitochondrial genome and paired amplified products exhibiting variations in SSCP profiles were cloned, reamplified, and rescreened by SSCP. For each of the cloned reamplified DNA products that demonstrated unique SSCP profiles, DNA sequencing was undertaken to identify the nature of the genetic changes.

Patients, Material, and Methods

Patient Characteristics

The study group consisted of 26 HIV-infected patients, of whom 16 received NRTI therapy. In the NRTI-treated group, 14 individuals were participants in clinical trials and were randomized to receive either stavudine and lamivudine (7 patients), zidovudine and lamivudine (4 patients), or stavudine and didanosine (3 patients), in combination with the HIV protease inhibitor indinavir (OzCombo I [$n = 11$]) or the nonnucleoside reverse-transcriptase inhibitor nevirapine (OzCombo II [$n = 3$]). Additionally, two patients were assessed who, after the introduction of ART, demonstrated clinical features of lipoatrophy (and are referred to as "symptomatic patients"), which was accompanied by the development of symptomatic hyperlactatemia in one patient and by the rapid enlargement of a subcutaneous hemangioma in the other patient. Ten HIV-infected ART-naive individuals were included as control subjects. (For patient demographics, see table 1.) Informed consent for the use of human genetic material was obtained from all individuals studied, and the study was approved by the Royal Perth Hospital ethics committee.

Sample Collection

In individuals participating in clinical trials, paired DNA samples were obtained from peripheral blood prior to ART (T1) and after an average of 24 mo on therapy (T2) (SD 12 mo, range 6–77 mo) (see table 1*A*). In patient 2, a pretreatment sample was unavailable because ART had been commenced interstate, so, in this case, the T1 sample was obtained after 12 mo of ART, with a 16-mo interval between the T1 and T2 samples. In the two symptomatic patients, samples were obtained prior to the commencement of therapy and after the development of symptoms (patient 15, 77 mo; patient 16, 47 mo). In the ART-naive patients, suitable paired blood samples were selected to control for the effect that HIV had on the levels of mtDNA mutations. In this group, time between paired samples averaged 41 mo (SD 23 mo, range 18–92 mo) (see table 1*B*).

mtDNA Study

Total genomic DNA was extracted from peripheral-blood samples obtained at T1 and T2, by conventional methods. A nested-PCR strategy was adopted, to amplify the entire mitochondrial genome. Initial amplification of six overlapping regions was achieved by long-range PCR, using primers designed to exclude known nuclear-encoded mitochondrial pseudogenes. Details of primer sequences are available on request. Long-range

PCR was performed using platinum Pfx DNA polymerase (Life Technologies) under the following amplification conditions: denaturation cycle at 94°C for 2 min; followed by 35 cycles of denaturation at 94°C for 15 s, annealing at 58°C for 30 s, and extension at 68°C at 1 min per kb; and then held at 4°C. These products were used as templates for second-round amplification in a series of 40 overlapping amplicons of ~400–800 bp.

Oligonucleotide primers were labeled with fluorescent HEX or FAM dyes and M-13 sequencing tags, to enable detection of the PCR products during SSCP and then during direct sequencing, respectively. The second-round amplification conditions were as follows: 1 cycle of denaturation at 95°C for 2 min; followed by 30 cycles of denaturation at 95°C for 20 s, annealing at 60°C–65°C for 45 s, and extension at 72°C for 90 s; and concluding with 1 cycle at 4°C for 1 min on a CR9600 Thermocycler (Corbett Research).

SSCP Analysis

Mutational screening was performed by SSCP analysis on the ABI 310 (Applied Biosystems) under conditions reported by Witt et al. (2000). In a typical assay, automated capillary electrophoresis was performed on the denatured amplified product (2 μl of PCR product, 10.5 μl of deionized formamide, 0.5 μl of 0.3-M NaOH, and 0.8 μl of GS 1000 ROX standard) that was injected at 15 kV for 5 s and was electrophoresed at 13 kV at 30°C for 30 min, using a 6% GeneScan polymer and the GeneScan buffer with EDTA. SSCP analysis within a capillary-gel-electrophoresis system was performed on the paired T1 and T2 samples, to screen for pattern differences reflecting sequence differences. The relative difference in mobility between the two products was visualized as distinct patterns in an output graph of the fluorescent intensity and relative molecular weight. The strand labeled with the FAM fluorophore consistently demonstrated informative patterns and was used to characterize the samples. Differences between interlane electrophoretic mobility of the DNA were normalized with GS 1000 ROX internal control within each sample and rarely exceeded 0.5 apparent molecular weight. SSCP patterns that diverged, between the paired samples, by >1.0 apparent molecular weight were considered to be different and to probably reflect sequence changes. Electrophoretic mobility varied between SSCP runs; hence, matched paired T1 and T2 samples were always included within an SSCP run.

Detection of Sequence Changes

Differences in DNA were identified by comparing the pattern of elution profiles of the amplified PCR products of the longitudinal samples. Those exhibiting differences in SSCP patterns were cloned, reamplified, and rescreened by SSCP. For the T1 and T2 samples, an example of each SSCP variant profile identified after cloning was sequenced, to determine the nucleotide differences associated with each of the altered SSCP profiles. For patient 1, two examples of clones with variant SSCP profiles were sequenced, and, in both examples, identical sequences were obtained. Thereafter, only a single example was sequenced.

pGEM Cloning

Cloning of the PCR product within the pGEM-T Easy system was performed under conditions recommended by the manufacturer (Promega). The transformants were selected, and the purified cloned DNA was used as a template for reamplification by the appropriate primers. The amplified cloned products were screened by SSCP analysis, to identify each DNA population. Randomly selected clones representative of each SSCP pattern were sequenced. To confirm that clones with identical SSCP profiles had identical DNA sequences, we initially sequenced two examples of clones from a T1 and T2 sample with identical SSCP patterns. In both examples, the sequences were identical.

Automated DNA Sequencing

The PCR products were purified using the Bresaspin PCR purification kit (Bresatec) and were sequenced using Dye Terminator sequencing chemistry on an ABI 373 DNA Sequencer (Applied Biosystems). Comparison and analysis were done using the MT Navigator software (version 1.0; Applied Biosystems).

Quantitative PCR for Measurement of mtDNA Copies/Cell

mtDNA and nDNA copy numbers were determined by a quantitative PCR assay using *Taq*man chemistry on the ABI 7700 Sequence Detection System platform (Applied Biosystems). To assess mtDNA content per cell, we measured the number of copies of a mitochondrial genome region (the 12S rRNA gene), normalized to a single-copy region of the nuclear-encoded human growth hormone (hGH) in independent reactions. Primer and probe sets used in the assay include the 12S rRNA gene (forward primer, 5′-TTG GAC GAA CCA GAG TGT AGC TT; reverse primer, 5′-TTA GCT CAG AGC GGT CAA GTT AAG; and probe, 6FAM-CAC AAA GCA CCC AAC TTA CAC TTA GGA GAT TTC A-TAMRA) and hGH (forward primer, 5′-TAT CCC AAA GGA CAG AAG TAT TCA TT; reverse primer, 5′-TTG TGT TTC CCT CCC TGT TGG A; and probe, VIC-5′-ACC TCC CTC TGT TTC TCA GAG TCT ATT CCG ACA-TAMRA). Fifty-microliter reactions were performed, containing 50 ng total DNA; 2.5 μM probe; 15 μM

Table 1

Characteristics of Longitudinal Samples

A. HIV-Infected Patients, before and after Initiation of ART

Patient/Sample	ART[a]	Time on Therapy (mo)	mtDNA Copies/Cell[b]	Identified mtDNA Region(s) with Sequence Changes	Lipoatrophy[c]
OzCombo I (n = 11):					
1/T1	Naive	0	289	…	No
1/T2	d4T/3TC/IND	49	121	Noncoding to 12S rRNA (nucleotides 220–1030)	Yes
2/T1	AZT/3TC/IND	12	nd	…	No
2/T2	AZT/3TC/IND	28	nd	Noncoding to 12S rRNA (nucleotides 220–1030)	No
3/T1	Naive	0	nd	…	No
3/T2	d4T/3TC/IND	24	nd	…	Yes
4/T1	Naive	0	106	…	No
4/T2	d4T/3TC/IND	25	83	…	No
5/T1	Naive	0	102	…	No
5/T2	d4T/3TC/IND	23	110	…	No
6/T1	Naive	0	nd	…	No
6/T2	d4T/3TC/IND	18	nd	…	No
7/T1	Naive	0	176	…	No
7/T2	d4T/3TC/IND	18	88	…	No
8/T1	Naive	0	75	…	No
8/T2	d4T/3TC/IND	6	116	…	No
9/T1	Naive	0	46	…	No
9/T2	AZT/3TC/IND	26	124	…	No
10/T1	Naive	0	93	…	No
10/T2	d4T/ddI/IND	40	148	…	No
11/T1	Naive	0	119	…	No
11/T2	d4T/ddI/IND	17	108	…	No
OzCombo II (n = 3):					
12/T1	Naive	0	135	…	No
12/T2	d4T/ddI/NVP	8	62	ND1 (nucleotides 3492–3750)	Yes
13/T1	Naive	0	79	…	No
13/T2	AZT/3TC/NVP	31	nd	…	No
14/T1	Naive	0	156	…	No
14/T2	d4T/3TC/NVP	19	61	…	No
15/T1	Naive	0	nd	…	No
Other (n = 2):					
15/T2	d4T/3TC/IND	77	nd	Noncoding (nucleotides 220–627),[d] COX I (nucleotides 6841–7276)	Yes
16/T1	Naive	0	172	…	No
16/T2	d4T/3TC/IND	47	135	COX III (nucleotides 9111–9635)	Yes

B. HIV-Infected, ART-Naive Patients (n = 10)

Patient	ART[a]	Time between Samples (mo)	mtDNA Copies/Cell[b]	Identified mtDNA Region(s) with Sequence Changes	Lipoatrophy[c]
17	Naive	33	nd	…	No
18	Naive	47	nd	…	No
19	Naive	22	nd	…	No
20	Naive	34	nd	…	No
21	Naive	42	nd	…	No
22	Naive	92	nd	…	No
23	Naive	73	nd	…	No
24	Naive	30	nd	…	No
25	Naive	18	nd	…	No
26	Naive	25	nd	…	No

[a] d4T = stavudine; 3TC = lamivudine; IND = indinavir; AZT = zidovudine; ddI = didanosine; NVP = nevirapine.
[b] nd = Not determined.
[c] Diagnosed on the basis of both percentage leg fat and criteria of Mallal et al. (2000).
[d] Although variant SSCP profiles between the T1 and T2 samples were observed within the noncoding region (nucleotides 220–627), identical profiles were detected within the overlapping amplicon (extending to nucleotide 1030); hence, the entire region (nucleotides 220–1030) was not cloned.

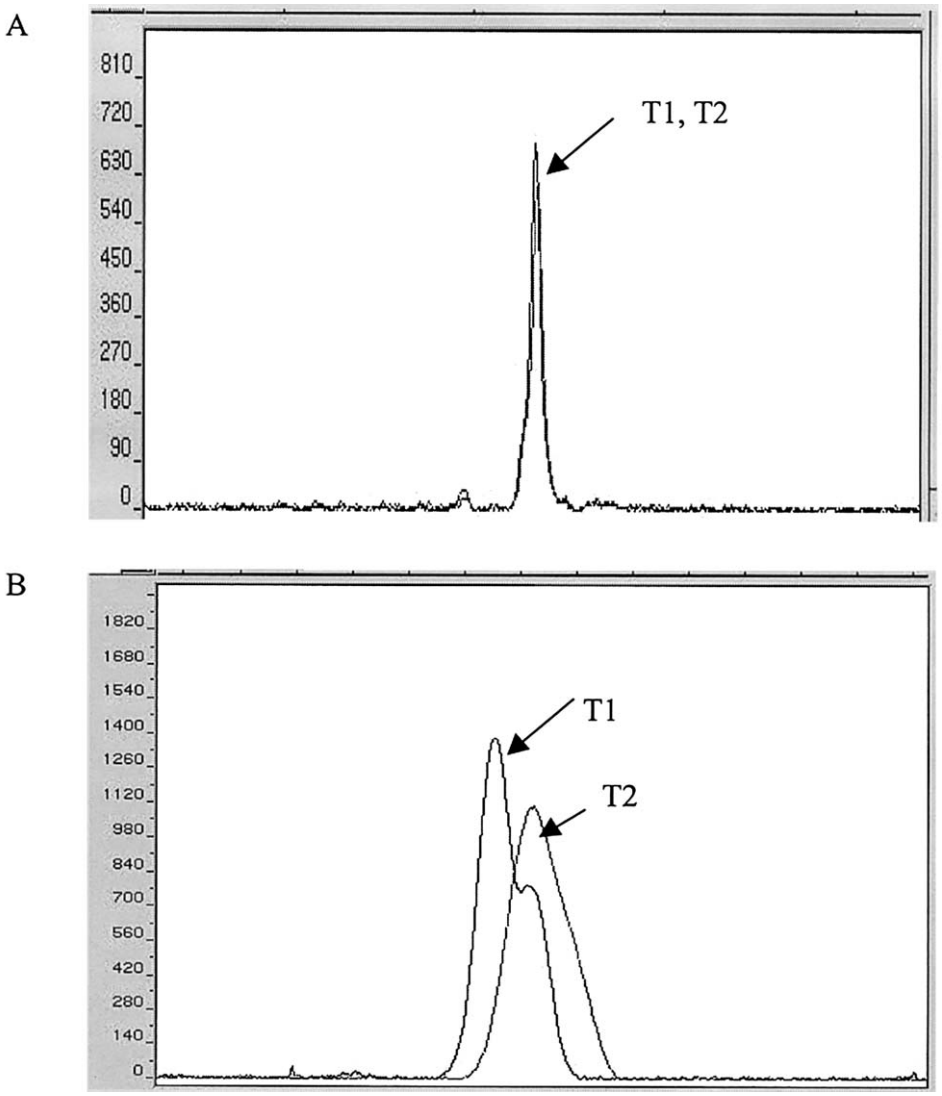

Figure 1 SSCP patterns in NRTI-treated individuals. *A,* Identical patterns between the pretherapy (T1) and posttherapy (T2) blood samples. *B,* Change in SSCP pattern on ART.

forward and reverse primers, respectively; and 2 × *Taq*man Universal Master mix (Applied Biosystems). The amplification conditions were similar for the two amplicons and included an initial cycle at 50°C for 2 min, followed by 1 cycle at 95°C for 10 min, and concluding with 45 cycles at 95°C for 15 s and 60°C for 1 min. The assay exploits *Taq*man technology, in which increased accumulation of PCR products is detected directly by increased fluorescence. The log of the input DNA is directly proportional to the number of amplifications required to generate a set level of fluorescence. Plasmid standards of known copy number were used in the assay, to derive the absolute quantities of mtDNA in the samples. The number of copies of mtDNA per cell was determined by normalization of mtDNA content to nDNA content through use of the following formula: $\log_{10}\text{mtDNA/cell} = \log_{10}\text{mtDNA} - \log_{10}\text{nDNA} - \log_{10}0.5$. Samples were run in duplicate, along with replicate controls, and assay performance was monitored using Shewhart plots, as reported by Hammond et al. (in press).

Statistical Analysis

Comparisons of mutational change and lipoatrophy outcome were performed using Fisher's exact test.

Results

Identification of Variant SSCP Patterns

Different SSCP patterns were observed between the paired amplicons from five NRTI-treated individuals (ta-

Table 2

Characterization of Heteroplasmic mtDNA Populations—from the Noncoding Region to 12S rRNA

Patient/Sample (No. of Clones Screened)	Pattern of Clones (% Similar)[a]	Heteroplasmic Nucleotide Positions (220–1030)[b]																											
		263G	275G	302A	309C	382G	398A	410A	431G	C[c]	466A	513C	522C	523A	524C	587A	601A	614A	624G	633A	697A	710C	740A	744T	756A	815A	825A	869C
1/T1 (27)	1 (78)	.	.	.	–	.	.	T	.	–	.	.	.	–	–	.	.	.	.	.	.	.	.	.	.	.	.	.	.
	2 (11)	.	.	.	–	.	.	T	.	–	.	.	.	–	–	.	.	.	.	G	.	.	.	.	.	.	.	.	.
	3 (11)	.	.	.	–	.	.	T	.	–	.	.	.	–	–	.	.	.	.	.	.	.	.	.	.	.	.	.	T
1/T2 (30)	1 (37)	.	.	.	–	.	.	T	.	–	.	.	.	–	–	.	.	.	.	.	.	.	.	.	.	.	.	.	.
	2 (33)	.	.	.	–	.	.	T	.	–	.	.	.	–	–	.	.	.	.	G	.	.	.	.	.	.	.	.	.
	4 (10)	A	.	G	–	.	.	T	.	–	.	.	.	–	–	.	.	.	.	.	.	.	.	.	.	.	.	.	.
	5 (7)	.	.	.	–	.	.	T	.	–	.	–	.	–	–	.	.	.	.	.	G	.	.	.	.	.	.	.	.
	6 (7)	.	.	.	–	.	G	T	.	–	.	.	.	–	–	.	.	.	.	.	.	T	.	.	.	G	.	.
	7 (3)	.	.	.	–	.	.	T	.	–	.	.	.	–	–	.	.	G	.	.	.	.	.	.	.	.	C	.
	8 (3)	.	.	.	–	.	.	T	.	–	G	.	.	.	.	.	.	.	.	.	.	.	.	.	.	.	.	.
2/T1 (13)	1 (100)	.	.	.	.	.	.	.	.	–	.	.	.	–	–	.	.	.	.	.	.	.	.	.	.	.	.	.
2/T2 (10)	1 (70)	.	.	.	.	.	.	.	.	–	.	.	.	–	–	.	.	.	.	.	.	.	.	.	.	.	.	.
	2 (10)	.	.	.	.	.	.	.	.	–	.	.	.	–	–	.	.	.	.	.	.	.	.	.	G	.	.	.
	3 (10)	.	.	.	.	.	.	.	.	C	.	.	.	–	–	.	G	.	.	.	.	T	.	C	.	.	.	.
	4 (10)	.	.	.	.	.	.	.	.	–	.	.	.	–	–	.	.	.	.	.	.	.	G	.	.	.	.	.
15/T1 (15)	1 (87)	.	C	.	.	C	.	T	.	–	.	.	.	.	.	.	.	.	A	nd	nd	nd	nd	nd	nd	nd	nd	nd
	2 (13)	.	C	.	.	C	.	T	A	–	.	.	.	.	.	G	.	.	A	nd	nd	nd	nd	nd	nd	nd	nd	nd
15/T2 (23)	1 (78)	.	C	.	.	C	.	T	.	–	.	.	.	.	.	.	.	.	A	nd	nd	nd	nd	nd	nd	nd	nd	nd
	3 (13)	A	C	.	.	C	.	T	.	–	.	.	.	.	.	.	.	.	A	nd	nd	nd	nd	nd	nd	nd	nd	nd
	4 (4)	.	C	.	.	C	.	T	.	–	.	.	.	.	.	.	.	.	T	nd	nd	nd	nd	nd	nd	nd	nd	nd
	5 (4)	.	C	.	.	C	.	T	.	–	.	.	–	–	.	.	.	.	A	nd	nd	nd	nd	nd	nd	nd	nd	nd
17/T1 (14)	1 (100)	nd	nd	nd	.	.	.	.	.	–	.	.	.	.	.	.	.	.	.	.	.	.	.	.	.	.	.	.
17/T2 (6)	1 (100)	nd	nd	nd	.	.	.	.	.	–	.	.	.	.	.	.	.	.	.	.	.	.	.	.	.	.	.	.

Note.—Nucleotide-sequence variation found in the cloned T1 and T2 samples was identified by examining the cloned insert by amplification, re-SSCP, and sequencing of the clones with unique SSCP patterns.

[a] SSCP pattern of clones (for details, see the "Results" section); the percentages of clones with similar patterns are given in parentheses.

[b] Except as otherwise noted, each subheading below gives a heteroplasmic nucleotide position and the corresponding nucleotide in the revised Cambridge reference sequence (GenBank accession number NC_001807). Within the table, dots (.) indicate identical to the reference sequence, and dashes (–) indicate deletion of a nucleotide; nd = not determined.

[c] Insertion of nucleotide C between nucleotides 440 and 441 of NC_001807 (GenBank), in patient 2.

Table 3

Characterization of Heteroplasmic mtDNA Populations—within ND1

Patient/Sample (No. of Clones Screened)	Pattern of Clones (% Similar)[a]	Heteroplasmic Nucleotide Positions (3492–3750)[b]							
		3527G	3532G	3539G	3619T	3676A	3684A	3704C	3746G
12/T1 (19)	1 (100)	.	.	.	.	.	.	.	C
12/T2 (18)	1 (78)	.	.	.	.	.	.	.	C
	2 (6)	.	.	.	.	.	G	.	C
	3 (6)	.	.	.	.	.	.	T	C
	4 (6)	.	.	.	C	G	.	.	C
	5 (6)	A	C	C	.	.	.	.	C
17/T1 (2)	1 (100)	.	.	.	.	.	.	.	.
17/T2 (2)	1 (100)	.	.	.	.	.	.	.	.

Note.—Nucleotide-sequence variation found in the cloned T1 and T2 samples was identified by examining the cloned insert by amplification, re-SSCP, and sequencing of the clones with unique SSCP patterns.

[a] SSCP pattern of clones (for details, see the "Results" section); the percentages of clones with similar patterns are given in parentheses.

[b] Each subheading below gives a heteroplasmic nucleotide position and the corresponding nucleotide in the revised Cambridge reference sequence (GenBank accession number NC_001807). Within the table, dots (.) indicate identical to the reference sequence.

ble 1*A;* e.g., see fig. 1*B*) in the following four regions: (1) noncoding to 12S rRNA (nucleotides 220–1030), in patients 1 and 2, and the noncoding region (nucleotides 220–627), in patient 15; (2) cytochrome oxidase subunit I (COX I) (nucleotides 6841–7276), in patient 15; (3) reduced-nicotinamide-adenine-dinucleotide dehydrogenase subunit 1 (ND1) (nucleotides 3492–3750), in patient 12; and (4) ATP6 to cytochrome oxidase subunit III (COX III) (nucleotides 9111–9635), in patient 16. mtDNA from paired samples, from most individuals on NRTI treatment (11/16) and all 10 therapy-naive patients, exhibited similar SSCP patterns before and after the interval period (table 1; e.g., see fig. 1*A*).

Variant profiles were observed in 3 of the 14 subjects enrolled in trials and in both of the symptomatic patients. In subjects with evidence of variant profiles, the interval between samples ranged from 8 mo (patient 12) to 77 mo (patient 15) (table 1*A*). Patients with variant profiles from OzCombo I trial (patients 1 and 2) received stavudine/lamivudine for 48 mo and zidovudine/lamivudine for 16 mo, respectively, and the patient from the OzCombo II trial was treated with stavudine/didanosine for 8 mo. One symptomatic individual (patient 15) received zidovudine/lamivudine/zalcitabine for 3 years, followed by stavudine/lamivudine (with indinavir) for 2 years (table 1*A;* previous drug therapy not shown). The remaining individual with lipodystrophy and hemangioma (patient 16) experienced significant enlargement of the hemangioma on zidovudine/lamivudine (and indinavir) therapy, although lipodystrophy had become clinically apparent during previous treatment with stavudine/lamivudine (and lopinavir). Patients were diagnosed with lipoatrophy or subcutaneous fat wasting, according to the criteria of Mallal et al. (2000) (table 1). Of the total of 26 patients who were examined in the present study, 4 of 5 patients with detectable mtDNA sequence changes during NRTI therapy also developed clinically apparent evidence of lipoatrophy, whereas lipoatrophy was present in only 1 of 11 patients without detectable mtDNA sequence changes. If we exclude the two nontrial patients who were included in the study *because* they became lipoatrophic on therapy, then the association between the development of fat wasting and the development of detectable sequence changes is significant ($P = .031$). One patient developed clinically apparent fat wasting without detectable sequence changes, while treated with NRTIs.

Analysis of the Cloned PCR Products to Identify Variant mtDNA Populations

The paired amplified products, across the four regions from the five patients, that showed initial SSCP screening differences were cloned, reamplified, and rescreened by SSCP, to identify the heteroplasmic population. For each of the reamplified cloned products exhibiting unique SSCP profiles, at least one example was sequenced, to identify the genetic changes responsible for conferring the unique profile. Details of the unique SSCP patterns and the number of clones exhibiting these patterns with the corresponding mtDNA sequence are shown for the four regions, as follows: from the noncoding region to 12S rRNA (table 2), within ND1 (table 3), within COX I (table 4), and from ATP6 to COX III (table 5). A substantial increase in the number of heteroplasmic mtDNA populations was observed

Table 4

Characterization of Heteroplasmic mtDNA Populations—within COX I

Patient/Sample (No. of Clones Screened)	Pattern of Clones (% Similar)[a]	Heteroplasmic Nucleotide Positions (6841–7276)[b]						
		7002A	7029T	7041T	7147A	7154T	7233C	7254A
15/T1 (17)	1 (82)	.	C	.	.	.	.	.
	2 (18)	.	C	.	.	.	.	G
15/T2 (14)	1 (50)	.	C	.	.	.	.	.
	3 (29)	.	C	C	.	.	.	.
	4 (14)	.	C	.	.	C	.	.
	5 (7)	G	C	.	G	.	T	.
17/T1 (7)	1 (100)	.	.	.	.	.	.	.
17/T2 (3)	1 (100)	.	.	.	.	.	.	.

Note.—Nucleotide-sequence variation found in the cloned T1 and T2 samples was identified by examining the cloned insert by amplification, re-SSCP, and sequencing of the clones with unique SSCP patterns.

[a] SSCP pattern of clones (for details, see the "Results" section); the percentages of clones with similar patterns are given in parentheses.

[b] Each subheading below gives a heteroplasmic nucleotide position and the corresponding nucleotide in the revised Cambridge reference sequence (GenBank accession number NC_001807). Within the table, dots (.) indicate identical to the reference sequence.

in T2 samples ($n = 27$) compared with T1 samples ($n = 11$) in the five NRTI-exposed patients in whom heteroplasmy was detected ($P = .042$, log rank).

In patient 1, the amplified products from the cloned pretherapy (T1) blood sample could be assigned to three SSCP patterns on the basis of the electrophoretic mobility of the products (tables 2–5). Of the clones, 78% exhibited a similar profile and were designated as "pattern 1," and 11% had a similar pattern that was distinct from pattern 1 and were designated as "pattern 2" (fig. 2*A*); pattern 3 (not shown) was also detected at a frequency of 11% of the T1-blood-sample clones (table 2). Multiple patterns were also detected in the T2-sample clones (tables 2–5). The common SSCP patterns (1 and 2) found in the T1-blood-sample clones were also common in the T2-sample clones, at frequencies of 37% and 33%, respectively (fig. 2*A*). SSCP pattern 3 was not observed within the T2 sample despite that 30 clones were analyzed. SSCP patterns 4, 5, and 6, detected in the posttherapy (T2) sample, were represented infrequently and were observed at levels of 10%, 7%, and 7% of clones, respectively (fig. 2*B*). SSCP patterns 7 and 8 (not shown) were detected at a frequency of 3% within the T2 DNA sample.

SSCP analyses of clones obtained from the five paired samples with variant SSCP profiles revealed evidence of heteroplasmic variants in T1 samples from three patients (tables 2, 4, and 5). In patients 1, 15, and 16, low-level heteroplasmic variants that were observed within the T1-

Table 5

Characterization of Heteroplasmic mtDNA Populations—from ATP6 to COX III

Patient/Sample (No. of Clones Screened)	Pattern of Clones (% Similar)[a]	Heteroplasmic Nucleotide Positions (9111–9635)[b]							
		9264A	9307T	9378G	9382C	9428C	9438A	9541C	9546A
16/T1 (19)	1 (85)	.	.	A	.	.	.	T	.
	2 (5)	.	.	A	T	.	.	T	.
	3 (5)	.	.	A	.	.	–	T	.
	4 (5)	G	C	A	.	.	.	T	G
16/T2 (15)	1 (86)	.	.	A	.	.	.	T	.
	2 (7)	.	.	A	T	.	.	T	.
	5 (7)	.	.	A	.	T	.	T	.
13/T1 (10)	1 (100)	.	.	.	.	.	.	.	.
13/T2 (6)	1 (100)	.	.	.	.	.	.	.	.

Note.—Nucleotide-sequence variation found in the cloned T1 and T2 samples was identified by examining the cloned insert by amplification, re-SSCP, and sequencing of the clones with unique SSCP patterns.

[a] SSCP pattern of clones (for details, see the "Results" section); the percentages of clones with similar patterns are given in parentheses.

[b] Each subheading below gives a heteroplasmic nucleotide position and the corresponding nucleotide in the revised Cambridge reference sequence (GenBank accession number NC_001807). Within the table, dots (.) indicate identical to the reference sequence, and dashes (–) indicate deletion of a nucleotide.

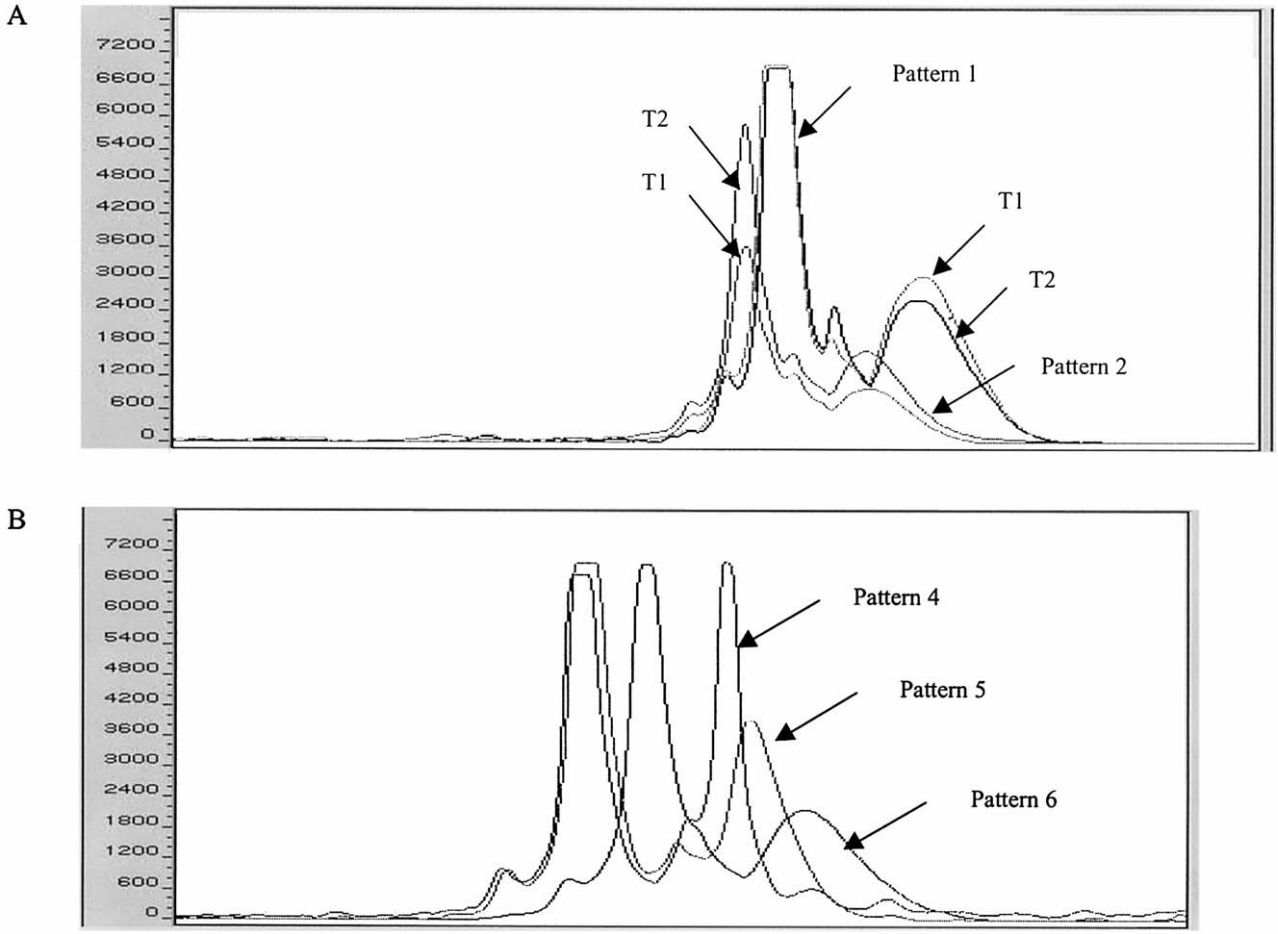

Figure 2 SSCP patterns in patient 1. *A*, Identical patterns (1 and 2) in the cloned T1 and T2 samples from patient 1. *B*, Examples of unique patterns (4–6), not found in the T1 sample, in the cloned T2 blood sample from patient 1.

sample clones were not detected within the T2 sample. In some patients (1 and 16), heteroplasmic populations identified in T1 samples either increased in frequency or were maintained at a similar level in the T2-sample clones. In all cases in which variant SSCP profiles were identified, however, novel heteroplasmic DNA populations were detected in T2 samples.

SSCP screening was performed on all 10 control samples, and identical SSCP profiles were obtained in the T1 and T2 samples. In addition, blood samples from an HIV-positive ART-naive individual (patient 17), obtained at T1 and after an interval of 33 mo, were used as a cloning control sample and were treated similarly. A single identical SSCP pattern was observed with the clones obtained from the paired samples, indicating the absence of detectable mutations associated with the amplification or the cloning technique (tables 2–4). Similarly, only one SSCP pattern was detected in the cloned T1 and T2 samples from NRTI-treated patient 13, in the region from ATP6 to COX III, providing additional evidence that the cloning procedure did not introduce sequence changes (table 5). No evidence of low-level heteroplasmy was observed in this patient.

Sequence Comparison of the Cloned Products

The mutations conferring the new SSCP patterns were identified by sequencing the mtDNA insert of one representative cloned sample with each unique pattern, and the sequences were compared with the reference sequence (GenBank accession number NC_001807). In all cases, each unique SSCP pattern of the cloned products correlated precisely with a unique sequence genotype (tables 2–5). For example, a sequence comparison of the clones obtained from the T2 sample from patient 1 indicate that the clones represented by SSCP patterns 4–8 are unique and each have at least two mutations when compared to the sequences obtained from the T1 sample. These mutations are not restricted to the noncoding region and are

Table 6

Nucleotide Substitutions Observed in the Cloned Samples from the mtDNA Regions (tRNA^{Phe}, 12S rRNA, ND1, COX I, and COX III)

Patient/Sample	Mutation/ Polymorphism	Codon Change[a]	Amino Acid Change	Synonymous?	Location[b]	Substitution[c]
1/T1	A633G	NA			tRNA^{Phe}	Transition
	C869T	NA			12S rRNA	Transition
1/T2	G263A	NA				
	A302G	NA				
	A398G	NA				
	A466G	NA				
	A614G	NA				
	A633G	NA			tRNA^{Phe}	Transition
	A697G	NA			12S rRNA	Transition
	C710T	NA			12S rRNA	Transition
	A815G	NA			12S rRNA	Transition
	A825C	NA			12S rRNA	Transversion
2/T1	…					
2/T2	A601G	NA			tRNA^{Phe}	Transition
	C710T	NA			12S rRNA	Transition
	A740G	NA			12S rRNA	Transition
	T744C	NA			12S rRNA	Transition
	A756G	NA			12S rRNA	Transition
15/T1	G431A	NA				
	A587G	NA			tRNA^{Phe}	Transition
15/T2	G263A	NA				
	A624T	NA			tRNA^{Phe}	Transversion
12/T1	…					
12/T2	G3527A	GCC-ACC	A74T	No	ND1	Transition
	G3532C	CCG-CCC	P75P	Yes	ND1	Transversion
	G3539C	GCT-CCT	A78P	No	ND1	Transversion
	T3619C	TTT-TTC	F104F	Yes	ND1	Transition
	A3676G	TCA-TCG	S123S	Yes	ND1	Transition
	A3684G	AAC-AGC	N126S	No	ND1	Transition
	C3704T	CTG-TTG	L133L	Yes	ND1	Transition
15/T1	A7254G	AAC-GAC	N451D	No	COX I	Transition
15/T2	A7002G	GTA-GTG	V366V	Yes	COX I	Transition
	T7041C	TAT-TAC	Y379Y	Yes	COX I	Transversion
	A7147G	ACT-GCT	T415A	No	COX I	Transition
	T7154C	ATA-ACA	M417T	No	COX I	Transversion
	C7233T	TAC-TAT	Y443Y	Yes	COX I	Transversion
16/T1	A9264G	ACA-ACG	T19T	Yes	COX III	Transition
	T9307C	TGA-CGA	W34R	No	COX III	Transition
	C9382T	CGC-TGC	R58C	No	COX III	Transition
	A9546G	GGA-GGG	G113G	Yes	COX III	Transition
16/T2	C9382T	CGC-TGC	R58C	No	COX III	Transition
	C9428T	CCT-CTT	P74L	No	COX III	Transition

NOTE.—Randomly selected clones of the paired samples were reamplified and screened by SSCP, to identify each genetic variant. The variants were sequenced and compared with the reference sequence (GenBank accession number NC_001807). The unique nucleotide substitutions, along with the predicted amino acid changes, are given.

[a] NA = not applicable (because the nucleotide substitution occurs in a non–protein-encoding sequence).

[b] tRNA^{Phe} and 12S rRNA extend from nucleotides 579–649 and 650–1603, respectively.

[c] Transitions are purine-purine or pyrimidine-pyrimidine substitutions; transversions are purine-pyrimidine or pyrimidine-purine substitutions.

present within the sequence encoding the tRNA^{Phe}, 12S rRNA, ND1, COX I, and COX III genes (tables 2–5).

Significance of the Nucleotide Substitutions within the mtDNA

For each of the five patients in whom heteroplasmy was demonstrated, nucleotide substitutions that were detected in the coding region within the T1 and T2 samples, compared with the consensus sequence, are described in table 6. Nucleotide substitutions that occurred in all the T1 and T2 cloned samples—for instance, nucleotide 3746C, in patient 12 (table 3), and nucleotide 7029C, in patient 15 (table 4)—although different from the consensus sequence, were considered to be inherited polymorphisms and are not included. A number of these substitutions are

unique and have not been reported before. Many have occurred at positions that result in a nonsynonymous substitution in the polypeptide. In the three patients (12, 15, and 16) in whom the rate of nonsynonymous substitutions could be assessed, there was a trend toward more nonsynonymous substitutions in the T2 sample ($n = 7$), compared with the T1 sample ($n = 3$). The levels of synonymous substitutions in these three patients were similar in the T2 samples ($n = 5$) and T1 samples ($n = 4$).

Measurement of mtDNA Copies/Cell

Levels of mtDNA copies/cell in blood samples were determined by quantitative PCR for 11 of the 16 patients who initiated NRTI therapy (table 1*A*). Of these 11 patients, 7 showed reduced levels of mtDNA in blood after initiation of therapy, including all those patients with evidence of mtDNA sequence changes on therapy for whom mtDNA depletion data was available.

Discussion

The results of this genomewide analysis of peripheral-blood mtDNA mutations in NRTI-treated individuals indicate that the use of these drugs provides conditions permissive for mutagenesis in vivo. The present study documents the emergence of heteroplasmic mtDNA populations in peripheral blood, providing evidence that novel mtDNA sequence variation can arise within individuals over a relatively brief period. Moreover, these data suggest that the acquisition of mtDNA mutations associated with NRTI therapy appears to be a dynamic process characterized by an increased generation of novel heteroplasmic populations, without evidence for positive selection of preexisting non–wild-type sequences.

The mtDNA mutations identified in the present study were identified by SSCP screening and subsequent DNA sequencing, to identify heteroplasmic positions. Confirmation required the presence of variant SSCP profiles and DNA sequences in clone populations. To exclude the possibility that mutations were generated during the amplification and cloning process, we also studied, as a control for cloning experiments, an HIV-positive, treatment-naive individual. The level of detection for heteroplasmic populations with SSCP and sequencing techniques was ~15% in our laboratory (data not shown), and we acknowledge that the presence of low-level heteroplasmy in the primary screen and also in other regions of the mitochondrial genome may have gone undetected. In this context, it is possible that the heteroplasmic mutant populations that were identified after the introduction of NRTI therapy were present, at a lower level, in treatment-naive samples. Nevertheless, in the present study, variant SSCP profiles in paired samples provided a highly specific screening tool for the identification of heteroplasmic mtDNA sequence differences between T1 and T2 samples. This approach may therefore provide a more broadly applicable genetic screening tool for the investigation of suspected mitochondrial diseases, utilizing paired samples in which a high degree of sequence homology is expected (i.e., within an individual or between matrilineally related individuals). Given the high degree of polymorphic diversity of the mitochondrial genome, in which coding-region sequence variation is frequent within and between ethnically distinct haplogroups (Herrnstadt et al. 2002), pathogenicity of a sequence variation may be suggested by its development over time in a symptomatic individual or by its presence in symptomatic tissues in comparison with unaffected tissues (Chinnery et al. 1999).

The results of the present study are consistent with a model in which upregulated cellular oxidative stress, accompanied by inhibition of protective DNA-repair mechanisms, results in an increased frequency of mtDNA point mutations. Coding and noncoding regions of the genome were affected, with no evidence for preferential accumulation of mutations either in specific regions or at sites associated with mitochondrial diseases. Additionally, NRTI therapy had no consistent effects on heteroplasmic mtDNA populations present prior to therapy, suggesting that polymerase-γ inhibition does not necessarily provide an advantage for variant mitochondrial sequences present before therapy. It is also notable that, although the present study was designed to detect sequence variants in the mitochondrial genome that result from substitutions and small-scale deletions or insertions, the presence of larger deletions (e.g., the 4,977-bp, "common" deletion) was not assessed. Hence, these data cannot provide additional insight into possible associations between NRTI drugs and the development of large-scale deletions. In this context, it has previously been suggested that truncated mtDNA templates may have a replicative advantage over wild-type sequences and are thus positively selected, in the presence of NRTI therapy (Wang et al. 1996; Lewis et al. 2001).

We conclude that NRTI therapy for HIV infection provides conditions permissive for the development of peripheral-blood mtDNA mutations in vivo, after 6–77 mo of drug exposure. The present study has shown that those NRTI-treated patients who developed sequence changes within mtDNA also showed decreased levels of mtDNA in blood on therapy. Further studies will be required in order to establish and elucidate the bioenergetic and pathophysiological consequences of these mutations, which may play a contributory role—along with mtDNA depletion—in the pathogenesis of mitochondrial toxicity associated with long-term NRTI therapy.

Acknowledgments

We acknowledge the services of Ms. Laila Gizzarelli and the DNA Sequencing Service at the Department of Clinical Immunology and Biochemical Genetics, Royal Perth Hospital, and the statistical expertise of Prof. Ian James and Ms. Susan Hermann, R.N. (Centre for Clinical Immunology and Biomedical Statistics, Murdoch University). The critical comments of Dr. Silvana Gaudieri are also appreciated. This project was supported by the Australian National Health & Medical Research Council (grant 194808).

Electronic-Database Information

The accession number and the URL for data presented herein are as follows:

GenBank, http://www.ncbi.nlm.nih.gov/Genbank/ (for the revised Cambridge reference sequence [accession number NC_001807])

References

Birkus G, Hitchcock MJ, Cihlar T (2002) Assessment of mitochondrial toxicity in human cells treated with tenofovir: comparison with other nucleoside reverse transcriptase inhibitors. Antimicrob Agents Chemother 46:716–723

Brinkman K, ter Hofstede HJ, Burger DM, Smeitink JA, Koopmans PP (1998) Adverse effects of reverse transcriptase inhibitors: mitochondrial toxicity as common pathway. AIDS 12:1735–1744

Chinnery PF, Howell N, Andrews RM, Turnbull DM (1999) Mitochondrial DNA analysis: polymorphisms and pathogenicity. J Med Genet 36:505–510

Hammond EL, Sayer D, Nolan D, Walker UA, de Ronde A, Montaner JSG, Cote HCF, Gahan ME, Cherry CL, Wesselingh SL, Reiss P, Mallal S. Assessment of precision and concordance of quantitative mitochondrial DNA assays: a collaborative international quality assurance study. J Clin Virol (in press)

Herrnstadt C, Elson JL, Fahy E, Preston G, Turnbull DM, Andersen C, Ghosh SS, Olefsky JM, Beal MF, Davis RE, Howell N (2002) Reduced-median-network analysis of complete mitochondrial DNA coding-region sequences for the major African, Asian, and European haplogroups. Am J Hum Genet 70:1152–1171

Johnson AA, Ray AS, Hanes J, Suo Z, Colacino JM, Anderson KS, and Johnson KA. (2001) Toxicity of antiviral nucleoside analogs and the human mitochondrial DNA polymerase. J Biol Chem 276:40847–40857

Kakuda TN (2000) Pharmacology of nucleoside and nucleotide reverse transcriptase inhibitor-induced mitochondrial toxicity. Clin Ther 22:685–708

Lewis W, Copeland WC, Day BJ (2001) Mitochondrial DNA depletion, oxidative stress, and mutation: mechanisms of dysfunction from nucleoside reverse transcriptase inhibitors. Lab Invest 81:777–790

Lewis W, Dalakas MC (1995) Mitochondrial toxicity of antiviral drugs. Nat Med 1:417–422

Longley MJ, Ropp PA, Lim SE, Copeland WC (1998) Characterization of the native and recombinant catalytic subunit of human DNA polymerase γ: identification of residues critical for exonuclease activity and dideoxynucleotide sensitivity. Biochemistry 37:10529–10539

Mallal SA, John M, Moore CB, James IR, McKinnon EJ (2000) Contribution of nucleoside analogue reverse transcriptase inhibitors to subcutaneous fat wasting in patients with HIV infection. AIDS 14:1309–1316

Martin JL, Brown CE, Matthews-Davis N, Reardon JE (1994) Effects of antiviral nucleoside analogs on human DNA polymerases and mitochondrial DNA synthesis. Antimicrob Agents Chemother 38:2743–2749

Palella FJ Jr, Delaney KM, Moorman AC, Loveless MO, Fuhrer J, Satten GA, Aschman DJ, Holmberg SD, HIV Outpatient Study Investigators (1998) Declining morbidity and mortality among patients with advanced human immunodeficiency virus infection. N Engl J Med 338:853–860

Wang H, Lemire BD, Cass CE, Weiner JH, Michalak M, Penn AM (1996) Zidovudine and dideoxynucleosides deplete wild-type mitochondrial DNA levels and increase deleted mitochondrial DNA levels in cultured Kearns-Sayre syndrome fibroblasts. Biochim Biophys Acta 1316:51–59

White AJ (2001) Mitochondrial toxicity and HIV therapy. Sex Transm Infect 77:158–173

Witt CS, Martin A, Christiansen FT (2000) Detection of *KIR2DL4* alleles by sequencing and SSCP reveals a common allele with a shortened cytoplasmic tail. Tissue Antigens 56:248–257